Classification: Biological sciences/Evolution

Structural color in *Junonia* butterflies evolves by tuning scale lamina thickness

Author affiliations:
Rachel C. Thayer[a] ORCID: 0000-0001-5856-7614
Frances I. Allen[b,c] ORCID: 0000-0002-0311-8624
Nipam H. Patel[a,d] ORCID: 0000-0003-4328-654X

[a]Department of Integrative Biology, UC Berkeley, Berkeley, CA 94720
[b]Department of Materials Science and Engineering, UC Berkeley, Berkeley, CA 94720
[c]California Institute for Quantitative Biosciences, UC Berkeley, Berkeley, CA 94720
[d]Marine Biological Laboratory, 7 MBL Street, Woods Hole, MA, 02543

Corresponding author: Rachel C. Thayer, University of California, Berkeley. Dept. of Integrative Biology.
thayerr(at)berkeley.edu.

Keywords:
Microevolution, macroevolution, thin film, optix, artificial selection, wing pattern, iridescence.

Abstract

Structural color is a pervasive natural phenomenon, caused by photonic nanostructures that refract light. Diverse organisms employ structural color to mediate ecological interactions and create specific optical effects such as iridescence. Despite its importance for living systems, the developmental, genetic, and evolutionary processes that generate structural color largely remain mysterious. Here, we focus on simple photonic structures, thin film reflectors, in the lower lamina of *Junonia* butterfly scales. We present multiple lines of evidence that the thickness of the lamina quantitatively controls lamina color, which is an important determinant of overall wing color, even when pigments are also present. First, in a lineage of buckeye butterflies artificially selected for blue wing color for 12 generations, a thicker lamina resulted in a color shift from brown to blue. A similar lamina thickness increase explains the appearance of blue scales in butterflies with mutations in the *optix* wing patterning gene. Finally, lamina thickness variation underlies the color diversity that distinguishes seasonal variants, sexes, and species throughout the genus *Junonia*. Thus, quantitatively tuning a single dimension of the existing scale architecture allows butterflies to evolve a broad spectrum of hues over both microevolutionary and macroevolutionary time frames. Because the lower lamina is an intrinsic component of typical butterfly scales, our findings imply that lamina structural color influences wing color in most butterflies.

Significance Statement

Structural colors, which result from photonic nanostructures that refract light and can create iridescence, are an important tool for many organisms. We use thin films, which are morphologically simple nanostructures that generate structural color in the lower lamina of butterfly scales, to dissect how photonic structures evolve. By combining interspecies comparisons with two different experimental approaches—artificial selection on wing color, and genetically engineered mutation of the *optix* wing patterning gene—we demonstrate that lamina thickness controls the wavelength (hue) of the structural color. These lamina structural colors are ubiquitous in the genus *Junonia,* and determine wing color along with pigments. Our results suggest that lamina structural colors probably exist in most butterflies, and that tuning lamina thickness facilitates wing color evolution.

Introduction

Structural colors are both visually delightful and abundant in nature. Organisms deploy structural colors to display hues for which they lack pigments (frequently blues and greens), to create specific optical effects such as iridescence or light polarization, and to mediate ecological interactions, including intraspecific signaling and camouflage. Unlike pigmentary color, which is caused by molecules that selectively absorb certain wavelengths of light, structural colors result from the constructive and destructive interference of light as it interacts with nanoscale, precisely-shaped physical structures that are made of a high refractive index material (e.g. keratin, chitin, or cellulose).

Despite the clear importance of structural color for living systems, the biological production of structural colors has long eluded characterization [1]. Many molecular techniques depend on harnessing variation to dissect biological processes, but color variation frequently confounds an array of structural and pigmentary components, and genetically isolating a single axis of structural variation can be challenging. Furthermore, photonic structures are submicroscopic in their entirety, and thus the magnitude of intraspecific variation in their dimensions is generally truly miniscule (e.g. tens of nanometers). Sheer smallness makes accurate measurement at the level of variation technically involved, particularly for high-throughput surveys of variation in populations, or over developmental time *in vivo*. While recent studies [2-4] have made early headway toward describing genetic regulation of structural colors, much work remains to decipher the evolutionary, developmental, and genetic bases of structural coloration, and lab-tractable systems with intraspecific variation in structural coloration are needed. We present a promising system, the butterfly genus *Junonia,* with extensive variation in a simple structural color, and show how structural simplicity is a tactical advantage toward unraveling how photonic structures are produced.

In butterflies, photonic nanostructures occur within the architecture of scales. Scales are the fundamental coloration unit on butterfly wings and have a Bauplan consisting of a grid of ridges and ribs, supported by a lower lamina that is a simple plane (Fig. 1A). Scales are composed of chitin and may also have embedded pigments. Intricate architecture and a high refractive index make scales a pliable substrate for photonic innovations, and indeed scales have been evolutionarily elaborated in many ways for impressive optical effects [5]. Even the simplest butterfly scales produce structural color, via the lower lamina acting as a thin film reflector. Thin films are the simplest photonic structure and consist of a layer of high refractive index material, on the order of 200 nm thick, surrounded by a material with a contrasting refractive index, i.e. air (Fig. 1B). Light is reflected from each surface of the film, and these two reflections interfere with each other. If the two reflections remain in phase, which depends on the extra distance traveled through the film and the wavelength, then they interfere constructively to produce observable color [6,7]. Conversely, wavelengths (colors) that undergo destructive interference have decreased brightness.

Here, we are able to test the role of lamina thickness in generating butterfly color by combining an artificial selection experiment, color mutants with disruptions in the *optix* wing patterning gene, and genus-wide associations between lamina thickness and wing color. We show that butterflies in the genus *Junonia* actively exploit the relationship between film thickness and color, using the thin films necessarily present in their scales to produce a broad spectrum of hues by tuning lamina thickness. These lamina colors work in tandem with pigments to define the wing pattern elements that distinguish populations, sexes, seasonal variants, and species, indicating that the ability to vary lamina thickness has been an important microevolutionary and macroevolutionary tool in this group, and likely in butterflies more broadly.

Results

Artificial selection for blue wing color increases lamina thickness

Here we describe a novel instance of rapid, artificially selected color shift from brown to blue wing color in *J. coenia* buckeye butterflies (Fig 1D-E) and identify the structural changes that enabled the color shift. Edith Smith, a private butterfly breeder, began selectively mating buckeyes with a few blue scales on the costal margin of the dorsal forewing (Edith Smith, personal communication). After five months of selective breeding, blue spread to the dorsal hindwing of some individuals. By eight months, there was a noticeable increase in blue surface area, and within roughly 12 months (on the order of 12 generations), most butterflies in the breeding colony were visibly blue over the majority of their dorsal wing surface. On the forewing, areas proximal to M1 were visibly blue, except the discal bars (Fig. S1). On the hindwing, blue shift did not include the distal-most wing pattern elements, i.e. EI-EIII and eyespots. At its strongest, the phenotype may include blue scales cupping the posterior forewing eyespot and/or a blue sheen in all distal elements of the forewing. Smith maintained the blue colony for several years, introgressing a few progeny from crosses to wild-caught buckeyes about once per year to maintain genetic diversity. Over time, she noted the emergence of a variety of short-wavelength colors, ranging from purple to green. Two years after focused selection, she estimated that the population was 85% blue, 8% green, 2% purple, and 5% brown. Like many familiar examples of human selection (e.g. domesticated animals, crop plants), outcomes are informative even without complete experimental documentation of the selective process [8,9]. These selected blue buckeyes provide a previously unexploited opportunity to study structural color. They demonstrate rapid and extensive evolutionary color change, and are a stark contrast to wild-type brown populations with which they are still interfertile. Conveniently, the artificially selected taxon, *J. coenia*, is a recognized model species for butterfly developmental genetics [10,11]. The selected blue individuals resemble naturally evolved color variants in the sister species, *J. evarete*, and offer a useful comparison to a previously reported artificial selection experiment in butterflies [12].

To pinpoint the cause of blueness in artificially selected butterflies, we characterized scales from the dorsal hindwing (Fig. 2A-D). When isolated and laid in the abwing orientation they occupy on the wing, cover scales were blue (Fig. 2B). However, when flipped over and viewed in adwing orientation, which exposes only the lower lamina, scales appeared more brightly blue and iridescence was more apparent (Fig. 2B', 2D). We tested whether the blue was structural rather than pigment-based by immersing the full scale in oil with a refractive index matched to that of chitin (Fig. 2B'''). Index-matching eliminates the possibility of refraction and structural color, leaving only pigment-based coloration. We measured the scale's absorption spectrum under these conditions (Fig. 3A), which revealed that blue scales did have some pigment, presumably a brown ommochrome [13], but this pigment cannot account for blueness. The pigment was mainly localized to the scale ridges. Lepidopteran structural colors may occur in the lamina, lumen, ridges, or cross-ribs. To isolate which of these features had the nanostructure responsible for blue structural color, we dissected the scales (Fig. 2B", Fig. S2 G). After removing all other scale components, we found that the bare lower lamina was sufficient for blue structural color. We also examined regions with all scale components except

150 the lamina and found that these pieces of lamina-less scale were not evidently blue (Fig. S2 H-
151 H" shows dissection minus the lamina for a *J. orithya* blue scale). We thus focused on
152 investigating nanostructure in the lamina. To discern between a single or multilayer lamina and
153 take precise measurements, we cross-sectioned the lamina and viewed it with Helium Ion
154 Microscopy (HIM) (Fig. 2C). HIM imaging indicated the lower lamina was a simple monolayer of
155 chitin with a thickness of 187 ± 13 nm (SD, Fig. 1C), which is a reasonable thickness to reflect
156 blue as a dielectric thin film [14].
157
158 We next investigated whether ground scales also contributed to blueness after artificial
159 selection. Butterfly wings have two classes of scales arranged in overlapping layers: superficial
160 cover scales and underlying ground scales. Cover and ground scales frequently have
161 contrasting size, shape, and color, and their juxtaposition can be important for wing color [14]. In
162 artificially selected buckeyes, the ground scales generally had similar architecture to the cover
163 scales, but with less uniform lamina color: ground scales exhibited a color gradient from the
164 stalk outward (Fig. S2 B'). Correspondingly, ground scales had a similar mean thickness but
165 more variability than cover scales (190 ± 29 nm). Ground scales were much more heavily
166 pigmented than cover scales (Fig. 3B), such that the abwing surface was black (Fig. S2 B). The
167 extra pigmentation in ground scales serves to enhance spectral purity by absorbing light
168 transmitted through the cover scales, thus reducing backscatter and making the observed blue
169 color more saturated (similar to [15]). We conclude that cover scale laminae are the major
170 source of blueness in artificially selected buckeye butterflies, while melanic ground scales
171 secondarily enhance spectral purity.
172
173 For comparison, we tested the source of color in wild-type brown scales and found that they
174 also had structural color (Fig. 2E-H). Brown cover scales had the same general architecture and
175 no more brown pigment than did blue cover scales—they had slightly lower mean pigmentation
176 than the selected blue scales, although the latter were more variable (Fig. 3A). The salient
177 difference was lamina thickness: brown scales were markedly thinner, measuring only 100 ± 5
178 nm (Analysis of Variance (ANOVA), $p < 2x10^{-16}$, Fig. 1C, Fig. 2G). A 100 nm chitin thin film
179 reflects a desaturated golden color due to reflectance of many long wavelengths. This golden
180 structural color was confirmed by the adwing scale color, the color of the bare lamina in
181 dissected scales, and the adwing reflectance spectra of brown scales (Fig. 2F'-F", H).
182 Therefore, though brown coloration is often attributed to pigmentation, wild-type brown cover
183 scales also had a structural color, one simply tuned to enhance different wavelengths.
184
185 Artificial selection also altered the absorption and lamina thickness of the ground scales. The
186 wild-type (brown) ground scales were thinner than the blue ground scales (140 ± 26 nm,
187 ANOVA, $p = 1x10^{-7}$). However, the mean difference was less extreme than in cover scales: blue
188 cover scales were on average 87 nm thicker than wild-type, while blue ground scales were on
189 average 50 nm thicker. Selected ground scales were markedly more absorbing than wild-type
190 ground scales (Fig. 3B, Fig. S2 D), which is consistent with increased pigmentation that
191 decreases backscatter in blue wing regions.
192

193 We conclude that the artificially selected buckeye butterflies rapidly evolved blue wing color via
194 an 87% mean increase in lower lamina thickness in cover scales and a similar but less
195 pronounced effect in ground scales. The effect was further amplified by increased pigmentation
196 in ground scales, but without removing brown pigment from cover scales. Our results show that
197 structural color can evolve quickly by modifying a single dimension of an existing structure, and
198 the process is facilitated by the initial presence of previously unrecognized structural color in
199 wild-type brown butterflies.
200
201 Since the artificially selected *J. coenia* wing pattern resembles natural iridescent variants in the
202 sister species, *J. evarete* (Fig 1F), we obtained hindwings of brown and blue *J. evarete*
203 individuals from different geographic locations and tested whether blue cover scales in this
204 species were also associated with increased lamina thickness (Fig. 2I-P). We found that the
205 same mechanism explained color differences between geographic color variants: blue scales
206 had 78% thicker scale laminae (blue 199 ± 14 nm; brown 112 ± 13 nm; ANOVA, $p < 2x10^{-16}$,
207 Fig. 1C) and no appreciable difference in pigmentation, compared to brown individuals (Fig.
208 3C). Furthermore, in blue *J. evarete*, the ground scales were darkly pigmented. Thus, the
209 artificially selected blue buckeyes faithfully recapitulate natural variation at the level of scale
210 coloration between sister species.
211
212 ***Color phenotypes in optix mutants include altered lamina thickness***
213 Recently, Zhang *et al*. used CRISPR/Cas9 to generate mosaic knockout mutants of *optix*, a
214 gene previously associated with pigment variation in butterfly wings [16]. Surprisingly, in
215 addition to pigmentation phenotypes, *optix* mutants in *J. coenia* gained blue iridescence in wing
216 scales. We tested phenotypically mutant blue scales from mosaic butterflies to determine how
217 structural and pigmentary changes control the color change (Fig. 2Q-T). Where blue scales
218 occured in the background region of the dorsal wing, color shift was due to the same factors
219 identified in artificially selected buckeyes. Lamina thickness of blue cover scales was
220 substantially increased compared to wild-type brown scales (212 ±11 nm, ANOVA, $p < 2x10^{-16}$,
221 Fig. 1C). The concentration of brown pigment in the cover scales was comparable to both wild-
222 type and selected animals (Fig. 3A). Ground scales were likewise similar to those of selected
223 blue animals, having thick and variable laminae (199 ±31 nm, ANOVA, $p=1x10^{-9}$ versus wild-
224 type. p=0.36 versus selected, Fig. 1C) and heavy pigmentation (Fig. 3B). Overall, blue scale
225 identity in *optix* mutants was caused by similar mechanisms as artificially selected blue. Our
226 analysis expands the initial mutant phenotype description by pinpointing its structural basis and
227 highlighting that the color shift depends on coordinated changes in both cover and ground
228 scales. Our findings also amend the conclusion that *optix* represses structural coloration in *J.*
229 *coenia* [16]. Rather, by regulating lamina thickness, *optix* regulates the wavelength of a photonic
230 structure that exists in both wild type and mutants. This distinction has implications for the likely
231 identities and behavior of downstream genetic factors, as well as the developmental basis of
232 mutant blue coloration. For example, rather than preventing a cascade of downstream genes
233 from acting to erect a photonic structure *de novo*, *optix* may subtly regulate the expression of a
234 gene or genes that directly regulate lamina thickness, such as chitin synthase.
235

236 *optix* knockout phenotypes also affected structural colors and pigments differently across wing
237 pattern elements. As originally reported, a pigment-specific effect was seen in regions of the
238 ventral wing of *optix* mutants where excess melanin was produced (Fig. S2 I-L). We also
239 observed regions where both pigment and structure were perturbed. For example, discal bars
240 on the dorsal forewing, which are normally orange, gained blue scales through both lamina
241 thickening and replacing orange with brown pigment (Fig. S2 M-P). In summary, *optix* knockout
242 can have varied effects in a single scale by altering pigment exclusively, structure exclusively, or
243 both in coordination. These findings are consistent with *optix*'s described role as a
244 developmental patterning gene that determines gross switches between discrete scale fates,
245 and which, directly or indirectly, can regulate diverse downstream factors [17]. Since appropriate
246 coloration critically depends on the proper combination of pigment and structural colors in both
247 cover and ground scales (e.g. [18,19]), it is of particular interest that *optix* can regulate all of
248 these components simultaneously. *optix* mosaic knockout mutants demonstrate that lamina
249 thickness can be experimentally perturbed and highlight a nimble candidate genetic pathway for
250 coordinated color evolution.
251
252 ***Lamina thickness consistently predicts structural color wavelength***
253 Relatives of *J. coenia* exhibit extensive color and pattern diversity, and blue structural colors in
254 particular show patterns of variation that hint at ecological relevance (e.g. sexual dichromatism,
255 seasonal polyphenism) (Fig. 4A). To assess the importance of lamina thickness variation in
256 macroevolutionary color diversity, we sampled cover scales from nine species in the genus
257 *Junonia* and a tenth species, *Precis octavia*, which belongs to the tribe Junoniini and exhibits
258 seasonally polyphenic wing coloration. We prioritized large pattern elements that distinguish
259 color forms within species. We compared scales using optical imaging, immersion index-
260 matching, spectrophotometry, and Helium Ion Microscopy. All scales sampled had typical
261 Nymphalid scale structure with a single plane of chitin forming the lower lamina, while
262 pigmentation was variable.
263
264 We tested whether the relationship between lamina thickness and color that we observed in
265 experimental contexts applies more broadly. We sought to address two questions: First, does
266 lamina thickness reliably predict lamina color, as measured from the adwing surface? While it is
267 well established that the thickness of a dielectric film controls the film's reflectance, other
268 variables such as refractive index, surface roughness, and pigmentation within the film also
269 factor into reflectance, and these could plausibly vary among taxa. Second, how variable is
270 lamina thickness? What range of thicknesses occur, and is there evidence for either quantized
271 or continuous thickness variation, or other biases that may reflect how the lamina forms during
272 scale development? To address these questions, we measured reflectance spectra from the
273 adwing surface of disarticulated cover scales from the 23 wing regions indicated in Fig. 4A. We
274 then cross-sectioned scales, imaged with HIM, and took thickness measurements.
275
276 We found that lamina thickness varied continuously between 90-260 nm, indicating that all
277 thicknesses over a more than 2.5-fold range are developmentally accessible (Fig. 5A). To better
278 visualize the relationship between thickness and lamina color, we clustered similar samples into
279 five color groups. Lamina colors in these groups could be described as gold, indigo, blue, and

green, with a fifth variable group that included magenta, copper, and reddish colored scales (labeled as “red” in Fig. 5). Thickness differed significantly between all color group pairwise comparisons (Fig. 5A, ANOVA: $p < 2x10^{-16}$, with *post hoc* Tukey’s Honestly Significant Difference test: $p < 2x10^{-6}$ for all pairwise comparisons). The color groups were also associated with different reflectance profiles (Fig. 5B). We obtained variable measures within individual specimens, which reflects biological color variation between adjacent scales, as well as varying color within individual scale laminae along their proximal-distal and lateral axes. *J. atlites* laminae were multicolored (Fig. 4G’), and thickness measures from this specimen overlapped the ranges of all color groups. The overall distribution of thickness was bimodal, with 110 and 180 nm films (i.e. gold and indigo) being frequent, and 150 and >240 nm films (i.e. red and green) less common.

Lamina thickness had a consistent relationship with adwing scale reflectance for the taxa and color range we sampled. The order of color shift as lamina thickness increased followed Newton’s series, which is the characteristic color sequence for thin films [6,21]. This sequence can be understood in terms of a sinusoidal thin film reflectance function, which shifts toward longer wavelengths as film thickness increases (Fig. 5C-G). The thinnest films appeared gold due to reflectance of all the longer wavelengths (Fig. 5C). In mid-thickness laminae, a mix of two oscillations determined color: reflectance of the first oscillation was shifted toward far red wavelengths, while a second reflectance peak rose in the ultraviolet (Fig. 5D). Visible reflectance of thicker laminae was dominated by the peak of the second oscillation as it moved from indigo to green (Fig. 5E-G). That the trend between thickness and reflectance holds broadly suggests that color changes in *Junonia* butterflies have recurrently evolved via lamina thickness adjustments. Moreover, the consistency of the relationship between thickness and reflectance is useful. For example, structural variation could be rapidly surveyed by extracting fitted thickness estimates from reflectance measurements, a much less laborious process than sectioning for electron microscopy.

Lamina structural color influences wing color throughout the genus Junonia

We next tested whether the extensive variation in lamina structural color among *Junonia* butterflies, explained by lamina thickness, also drives overall wing color. Compared to reflectance from the adwing lamina surface, wing color integrates many more factors, such as scale stacking and density. In particular, since the the abwing scale surface faces outward on the wing, wing color is weighted heavily by pigments localized in the ridges on cover scale abwing surfaces. We measured pigmentation in cover scales from the same regions (Fig. 4A) to assess whether pigments or lamina structural color better explained wing color. Structural color of the lamina influenced wing color, although the strength of this influence was modulated by pigments. Specimens generally fit three categories: 1) only structural color involved, 2) structure and pigment were coordinated, 3) structure and pigment were discordant. We present representative specimens in these categories (Fig. 4B-M”). (Structural colors and pigments are listed per specimen in Table S1.)

First, in a number of wing regions the lower lamina appeared to be the sole determinant of overall color. For example, the cover scales in the blue basal aura regions of male *J.*

westermanni, *J. hierta*, and *J. oenone* wings had blue laminae and lacked pigment (Fig. 4B-C”). Spectral purity in basal auras was also enhanced by underlying ground scales with high melanin content. Most of the unpigmented scales we sampled were blue, with the notable exception of *J. atlites* scales (Fig. 4F-G”). These scales had rainbow graded laminae, which presumably create the overall light grey by additive color mixing [22]. *J. atlites* demonstrates that lamina structural color can be fundamental even in neutrally colored wing regions that are not obviously iridescent, and also that thickness can be patterned at fine spatial resolution within a single lamina.

The second category, scales with coordinated structural and pigment colors, is typified by yellow scales from *J. hierta* (Fig. 4D-E”). These scales combined a yellow lamina color with limited yellow pigment that waned toward the proximal tip of the scale (which is generally obscured by the neighboring row of scales on the wing). Here the pigment and structural color were mutually reinforcing, with the lamina sensibly reflecting wavelengths that the pigment does not absorb.

Even in scales where pigmentary and lamina structural colors were discordant, lamina color appeared to influence wing color. Several wing regions had colored laminae dampened by a neutral dark pigment (i.e. a pigment that absorbs all visible wavelengths). This included scales like those of *J. coenia* and *J. evarete*, where wing color was due to reflected light from the lower lamina, but brightness was attenuated by brown pigment in the ridges and ribs (Fig. 2). Perhaps dark pigment in the ridges also acts like a Venetian blind to limit iridescence, so that at high viewing angles, where iridescence would be strongest, light from the lamina is quenched. We also observed blue laminae mismatched with red pigments in female *J. westermanni* and the wet season form of *P. octavia*. When viewed at high resolution, both red and blue colors were obvious in wet season *P. octavia* scales (Fig. 4J-K”). Red pigment was localized to the ridges and ribs, and reflected blue light from the lower lamina spilled through the windows between them. Since the wing appears red when viewed macroscopically, blue laminae were unexpected. For perspective on the optical function of blue laminae in this context, we compared the discordant red scales with scales from the band that remains red in both *P. octavia* seasonal forms (Fig. 4L-M”). The latter were a more intense red than scales from outside the band, due to both increased red pigment and laminae that were better coordinated: lamina colors in these scales included copper and magenta (Fig. 4M’). Optically, underlaying red pigment with a blue lamina contributes to a less saturated red. Red scales show that butterfly wing color can be determined by complicated mix-and-matching of different lamina thicknesses and pigment deposition. Discordant scales also convey that although having a lower lamina is architecturally necessary in butterfly scales, its color properties may at times be an optical liability, counteracted by pigmentation.

Comparison to thin film equation

We compared our empirical data to Fresnel’s classical thin film equations, which model the reflectance of an idealized dielectric thin film [7,23]. This model has previously been used to estimate the thickness of butterfly scale laminae based on their adwing reflectance spectra [14,19]. For each sample, we modeled the expected reflectance using our thickness measurements, and then compared to the measured reflectance spectra. We used 1.56 for the

refractive index of chitin [24] and a maximal angle of illumination of 30.2° following [25] (because spectra were measured through an objective lens with a numerical aperture of 0.5). To account for measurement error, we modeled films over all thicknesses within one standard deviation of the measured mean per sample (red envelopes, Fig. S3 A). We also modeled films with Gaussian thickness distributions for each sample, following [15]. This model is analogous to a single uneven film with mean thickness and surface roughness defined by the measured thickness and sample standard deviation (solid red lines, Fig. S3 A). We found that qualitatively the model describes the main behaviors of our data: reflectance oscillates with a given frequency and brightness, and the function shifts toward longer wavelengths as thickness increases. Quantitatively, mean maxima and minima in the reflectance function were offset laterally for every specimen, by about 40-80 nm, with the modeled curves blue-shifted relative to the observed. A similar blue shift has been reported in butterfly scale laminae before [12]. The comparison improves if we assume a higher refractive index or thickness. However, to align modeled and measured spectra would require either an impossibly high refractive index (around 1.75) or increased thickness outside the error range of our measures (20-25 nm thicker than mean measurements). Possibly the lateral offset is due to a combination of the former. Alternatively, these results could indicate that scales have additional properties not fully described by the model. There are a number of differences between the idealized film and real scales, including curvature of the film, pigmentation, and fluctuations in thickness. The lamina itself may not necessarily have a uniform material composition or refractive index. For example, contrasting sublayers within the lamina (as in [26]) could create extra reflective interfaces. Thus, our data are compatible with the expected behaviors of thin films, but modeling the specific case of butterfly scale laminae with quantitative precision may require additional parameters or calibration to an empirical dataset.

Discussion

We used both interspecies comparisons and two different experimental approaches (artificial selection on wing color and knockout of the *optix* locus) to show that lower lamina thickness quantitatively controls structural color of the lamina in butterfly scales. This relationship matches Newton's color series for dielectric thin films and holds for both pigmented and unpigmented scales. To put this finding in context, we show that lamina structural color is, in turn, an important determinant of overall wing color, including in wing regions that are neutral (e.g. brown, grey) or long-wavelength (e.g. red, yellow) colors. Lamina structural colors contribute to the color differences among seasonal variants, sexes, species, and selectively-bred lineages of *Junonia* butterflies, highlighting that quantitatively tuning lamina thickness is a vehicle for color evolution in both micro and macroevolutionary contexts. Lamina thickness is highly variable in *Junonia*, ranging from 90-260 nm, which results in a broad spectrum of lamina structural colors produced in wing scales that can be accentuated or muted by pigments. We also find that in addition to its known role in regulating pigments, the *optix* locus can regulate lamina thickness in both cover and ground scales, confirming its utility for coordinated color evolution.

Because the lower lamina is part of the typical architecture of butterfly scales, our findings have broad implications for future research on adult color in numerous butterfly taxa. Foundational

literature drew a distinction between highly derived scales with vivid structural colors and "standard, undifferentiated scales," which conform to the butterfly scale Bauplan, have a simple monolayer lower lamina, and "are not truly iridescent, i.e., they do not produce brilliant structural colors" [27]. However, within the past ten years, individual examples of thin film interference from the lower lamina have emerged in diverse Lepidoptera, including in simple scales [12,14,15,19,26,28,29]. Our thorough examination of many simple scales shows that thin film interference is a ubiquitous component of wing color. Reflectance from the lower lamina is likely present in all scales that resemble the scale Bauplan, meaning that lamina structural colors presumably play a role in most butterfly scales, and likely arose very early in butterfly evolution. Because it appears to be typical that butterflies produce multiple lamina colors across wing pattern elements and scale types, it is probable that the developmental genetic networks for quantitatively varying lamina thickness are deeply conserved as well. Hence, it will be useful to report which lamina colors are present, in addition to identifying pigments, when describing butterfly colors.

We can now draw comparisons about the process of evolutionarily modifying structural color. There are several striking similarities between this study and, to our knowledge, the only other reported artificial selection on butterfly wing color, by Wasik *et al.,* which selected for violet structural color in *Bicyclus anynana* [12]. Since the selected taxa, *J. coenia* and *B. anynana*, diverged 78 million years ago, [30] these similarities may be informative about evolvability in nymphalid butterflies generally. In both cases, color shift was accomplished by modifying the dimension of an existing structure: the lower lamina. Given the short timescale of these studies, this is unsurprising, although clearly novel structures are ultimately possible. Both studies observe a rapid (8-12 generations) and pronounced (46-87%) increase in lamina thickness that was the essential cause of color shift, with pigmentation being less important. There are also intriguing differences. The selection we describe primarily affected cover scales, whereas Wasik *et al.* reported that the primary structural effect was in ground scales, which is surprising, since increasing thickness in the obscured ground scales has less impact on wing color. There may be a difference in available standing genetic variation in cover versus ground scale lamina thickness between the two taxa. Since less light from ground scale laminae escapes the wing, ground scale laminae may be subject to less constraint and therefore frequently harbor more standing variation in thickness than cover scales. By contrast, selection in *J. coenia* likely exploited elevated cover scale thickness variation from the outset. Selection began with individuals that already had a few blue cover scales. Moreover, *J. coenia* is known to be interfertile with *J. evarete,* [31] which can be blue, and the two co-occur in Florida where selection occurred, making allele introgression a possible source of genetic variation. Differences of magnitude notwithstanding, both scale types did thicken in both studies; it is unclear whether thickness gains in both are parallel responses, or whether a change in one scale type pleiotropically shifts the other.

Physical constraints inherent to thin film colors may help explain the division of color space between pigments and structures. It is not fully understood why certain hues seem to be more often produced by pigments while others are more often produced by structural colors (e.g. the abundance of blue structural colors but lack of blue pigments in birds [32] and the rarity of red

structural color in birds and beetles [33]). In *Junonia,* we show that by tuning thickness, thin film laminae can produce nearly all the spectral colors (i.e. yellow, green, blue, indigo), and even light achromatic colors (e.g. light grey) via color mixing across a gradient. Yet thin films are fundamentally incapable of producing certain colors, notably dark brown, black, and pure red. The medium thickness films that most nearly approach red have inherently poor color properties due to the oscillating nature of thin film reflectance spectra. First, since the colors of mid-thickness films are a mix of two reflectance peaks (Fig. 5C), they are reddish but not pure or well-saturated, and are better described as copper, magenta, and purple. Further, mid-thickness films are not bright: they reflect less total visible light than other thicknesses we observed (compare Fig. 5D to 5C, E-G). By contrast, red, black, and brown are prevalent pigment colors in *Junonia*, making pigments and thin film structural colors complementary color palettes with little overlap. The optical limitations of thin films may have partially determined how pigment families and scale architecture evolved in early butterfly lineages, which in turn initialized whether pigments or structures provide the most accessible route to evolve a given hue during subsequent diversification.

Color evolvability in butterflies is also a function of the genetic architecture that regulates color. We have shown that *optix* knockout alters lamina colors and pigments in both ground and cover scales, and that these outcomes vary across the conserved wing pattern elements that comprise the Nymphalid ground plan [34]. Thus, the *optix* pathway appears to integrate many upstream patterning inputs and translate them into an array of coordinated outputs. By maintaining synergistic pigment and lamina color pairings across scale types, the *optix* pathway effectively reduces the genetic distance between these coordinated color combinations, which likely helps butterfly taxa efficiently reach new optimums. Our artificial selection results also provide evidence that selective responses can proceed via discrete jumps like those induced by *optix* mutations. During selection, blue wing surface area increased over generational time, but there was no intermediate stage of reddish butterflies, as would be seen if lamina thickness increased linearly. Further investigation of the topology, regulation, and evolution of the *optix* network will enhance our understanding of the production of thin film reflectors and their role in butterfly wing color.

In summary, thin film reflectors, a morphologically simple class of photonic structures, are experimentally manipulable and broadly employed in the lower lamina of butterfly wing scales. Lamina thickness explains variation in structural color wavelength, responds to selection on wing color, and can be regulated by the *optix* wing patterning gene. Tuning lamina thickness facilitates both microevolutionary and macroevolutionary shifts in wing color patterning throughout the genus *Junonia*. The buckeye butterflies are a promising study system with which to decipher the genetic and developmental origins of structural color.

Materials and Methods

Butterfly specimens

Artificially selected blue *J. coenia* were purchased as larvae from Shady Oak Butterfly Farm in 2014 (Brooker, FL, USA) and reared on fresh *Plantago lanceolata* at 27-30 °C on a 16/8 hour day/night cycle. We acquired preserved specimens from various vendors and collaborators (Table S1). Species-level identification was generally unambiguous. However, relationships among Neotropical *Junonia* are not well-resolved, their historical designations are convoluted, and the limited molecular data available do not cleanly support current designations [35-37]. Two recognized species, *J. evarete* and *J. genoveva*, have large ranges with extensive overlap and many variable color forms, including both brown and blue. We therefore described three Neotropical specimens as belonging to the *J. evarete* species complex to avoid accidental misidentification. Available diagnostic details, including ventral antenna club color, are in Table S1.

Optical Imaging

Scales were laid on glass slides. Optical images of scales were taken with a Keyence VHX-5000 digital microscope (500-5000x lens). For refractive index matching, we used Cargille Laboratories immersion oil (nD=1.56), and imaged with transmitted light. Scales were dissected by hand using a capillary microinjection needle. Whole wings were also imaged on the Keyence VHX-5000, using the 20-200x lens.

Microspectrophotometry

For reflectance spectra, individual scales were laid flat on a glass slide, with the adwing surface facing up. We collected spectra with an Ocean Optics Flame-S-UV-Vis-Es spectrophotometer mounted on a Zeiss AxioPhot reflected light microscope with a 20x/0.5 objective and a halogen light source. Measurements were normalized to the reflectance of a diffuse white reference ($BaSO_4$, Carolina). Data were recorded with SpectraSuite 1.0 software, with 3 scans to average and boxcar width of 7 pixels. We allowed the software wizard to determine optimal integration time using the reference sample; time was generally about 7 milliseconds. Spot size was roughly circular, 310 μm in diameter, and centered on the scale. We processed spectra in RStudio 1.0.153 with the package ‘pavo,’ version 0.5-4 [38]. We first smoothed the data using the *procspec* function with *fixneg* set to zero and *span* set to 0.3. We then normalized the data using the “minimum” option of the *procspec* function, which subtracts the minimum from each sample. Because we use a diffuse standard and scales are specular, raw spectra overestimate reflectance. We therefore followed [14] in dividing spectra by a correction factor. We used a smaller correction factor of only 2.5, because in our setup the scale does not fill the full field of view. Absorption spectra from scales submerged in index-matched oil were collected and processed similarly, but under transmitted light with an integration time of 0.01 seconds, and without the “minimum” option.

Helium Ion Microscopy

Surface imaging by HIM provides increased depth of field and enhanced topographic contrast compared to Scanning Electron Microscopy, as demonstrated for a range of biological and other

materials [39], including butterfly wing scales [40]. Samples were prepared for HIM by laying the wing on a glass slide with the region of interest facing down, wetting with ethanol, and freezing with liquid nitrogen. We then promptly cross-sectioned the wing through the region of interest by hand with a new razor blade. After the sample warmed and dried, we used a capillary microinjection needle to transfer individual cut scales onto carbon tape. Scales were placed overhanging the edge of a strip of carbon tape, with one end pressed into the tape for good contact. We optically imaged the tape strip as a color reference, and then transferred the tape to the vertical edge of a 90° stepped pin stub (Ted Pella #16177). While non-conductive samples can be imaged by HIM using low energy electrons for charge neutralization (a key benefit of HIM for bio-imaging), we found that the unsupported overhanging edges of our scales tended to bend due to local charging [41]. We thus sputter coated with 4.5 - 13 nm of Au-Pd using a Cressington 108auto or Pelco SC5. Images (secondary electron) of the sectioned scales were acquired with a Zeiss ORION NanoFab Helium Ion Microscope using a beam energy of 25 keV and beam current of 0.8 - 1.8 pA (10 µm aperture, spot size 4). Even with vertical mounting, the sectioned surface was not always perfectly perpendicular to the direction of the imaging beam, largely due to the scales' tendency to curve. Viewing angle is critical, since measurements taken from a projected image viewed under erroneous tilt could cause systematic underestimation of thickness. We therefore tilted the microscope stage until the scale lamina was perpendicular at the measurement site, as diagnosed by observing an inflection point in lamina curvature (i.e. a switch between the upper and lower surfaces being visible). We performed a tilt calibration to test the precision of our inflection point criterion and determined that an inflection point was only visible if the sample was within 4-5° of perpendicular (Fig. S4 B-D). Since erroneous tilt is limited to 5°, thickness underestimation is limited to 1 nm. Slight overestimations are likely, due to the sputter coating. Using the line measurement tool in ImageJ software, we measured lamina thicknesses only at visible inflection points. We corrected measurements for slight variations in working distance not accounted for by the software scale bar, using $T_{correct} = (T_{raw})/9058$ µm x d µm, where d is the measured working distance and 9058 µm is the reference working distance. Thickness of female *J. westermanni* scales was not measured, because specimens were unavailable. The sectioned scale shown in Fig. 1A was milled using the gallium ion beam of the Zeiss ORION NanoFab (beam energy 30 keV, beam current 300 pA).

Modeling film thickness

We modeled the reflectance from chitin thin films as previously described [25], including integrating reflectance for values of θ from zero to the maximal angle of illumination (i.e., averaging reflectances to simulate the inverted cone of light collected, given the numerical aperture of the objective lens used in microspectrophotometry). Specifically, since our objective had NA=0.5, we first calculated reflectance over values of θ from 0 to 30.2°, multiplied each by 2πθ, and then averaged over the cumulative circular surface area. For the model with Gaussian thickness distributions, we followed [15] using n=400 observations from the simulated thickness distribution.

Acknowledgements

We thank Linlin Zhang and Robert Reed for *optix* mutant wings; Masaki Iwata and Joji Otaki for *J. orithya* wings; and Krushnamegh Kunte for the image of female *J. hierta*. We thank Edith Smith for fantastic blue buckeyes, information about their origin, and the image in Fig. 1E. We are indebted to Ryan Null, Bodo Wilts, and Samuel Thayer for insightful discussions. Erika Anderson, Craig Miller, and Michael Nachman read the manuscript. Helium Ion Microscopy was performed at the Biomolecular Nanotechnology Center, a core facility of the California Institute for Quantitative Biosciences, University of California, Berkeley. Funding was provided by a National Science Foundation Doctoral Dissertation Improvement Grant DEB-1601815 (to R.C.T. and N.H.P.) and a National Science Foundation Graduate Research Fellowship DGE-1106400 (to R.C.T.).

References

1. Cuthill IC, et al. (2017) The biology of color. *Science* 357(6350):eaan0221.

2. Parnell AJ, et al. (2018) Wing scale ultrastructure underlying convergent and divergent iridescent colours in mimetic Heliconius butterflies. *J Royal Soc Interface* 15(141):20170948.

3. Matsuoka Y, Monteiro A (2018) Melanin pathway genes regulate color and morphology of butterfly wing scales. *Cell Reports* 24(1):56–65.

4. Brien MN, et al. (2018) Phenotypic variation in Heliconius erato crosses shows that iridescent structural colour is sex-linked and controlled by multiple genes. *J Royal Soc Interface Foc* 9(1):20180047.

5. Ghiradella H (1985) Structure and development of iridescent lepidopteran scales: the Papilionidae as a showcase family. *Ann Entomol Soc Am* 78(2):252–264.

6. Mason CW (1927) Structural colors in insects. II. *J Phys Chem* 31(3):321–354.

7. Yeh P (2005) *Optical waves in layered media* (John Wiley, Hoboken).

8. Akey JM, et al. (2010) Tracking footprints of artificial selection in the dog genome. *Proc Natl Acad Sci* 107(3):1160–1165.

9. Wright SI, et al. (2005) The effects of artificial selection on the maize genome. *Science* 308(5726):1310–1314.

10. Carroll SB, et al. (1994) Pattern formation and eyespot determination in butterfly wings. *Science* 265(5168):109–114.

11. Nijhout HF (1980) Ontogeny of the color pattern on the wings of Precis coenia (Lepidoptera: Nymphalidae). *Dev Biol* 80(2):275–288.

12. Wasik BR, et al. (2014) Artificial selection for structural color on butterfly wings and comparison with natural evolution. *Proc Natl Acad Sci USA* 111(33):12109.

13. Nijhout HF, Koch PB (1991) The distribution of radiolabeled pigment precursors in the wing patterns of nymphalid butterflies. *J Res Lep* 30(1–2):1–13.

14. Stavenga DG, Leertouwer HL, Wilts BD (2014) Coloration principles of nymphaline butterflies: Thin films, melanin, ommochromes and wing scale stacking. *J Exp Biol* 217(12):2171–2180.

15. Siddique RH, Vignolini S, Bartels C, Wacker I, Hölscher H (2016) Colour formation on the wings of the butterfly Hypolimnas salmacis by scale stacking. *Scientific Reports* 6(1):36204.

16. Zhang L, Mazo-Vargas A, Reed RD (2017) Single master regulatory gene coordinates the evolution and development of butterfly color and iridescence. *Proc Natl Acad Sci* 114(40):10707–10712.

17. Martin A, et al. (2014) Multiple recent co-options of Optix associated with novel traits in adaptive butterfly wing radiations. *EvoDevo* 5(1):7.

18. Wilts BD, Pirih P, Stavenga DG (2011) Spectral reflectance properties of iridescent pierid butterfly wings. *J Comp Phys A* 197(6):693–702.

19. Wilts BD, Vey AJ, Briscoe AD, Stavenga DG (2017) Longwing (Heliconius) butterflies combine a restricted set of pigmentary and structural coloration mechanisms. *BMC Evo Biol* 17(1):226.

20. Kodandaramaiah U (2009) Eyespot evolution: phylogenetic insights from Junonia and related butterfly genera (Nymphalidae: Junoniini). *Evol Dev* 11(5):489–497.

21. Shevtsova E, Hansson C, Janzen DH, Kjærandsen J (2011) Stable structural color patterns displayed on transparent insect wings. *Proc Natl Acad Sci* 108(2):668–673.

22. Vukusic P, Kelly R, Hooper I (2009) A biological sub-micron thickness optical broadband reflector characterized using both light and microwaves. *J Royal Soc Interface* 6(Suppl 2):S193–S201.

23. Fresnel AJ (1834) *Mémoire sur la loi des modifications que la réflexion imprime à la lumière polarisée* (De l'Imprimerie de Firmin Didot Frères ..., Paris).

24. Vukusic P, Sambles JR, Lawrence CR, Wootton RJ (1999) Quantified interference and diffraction in single Morpho butterfly scales. *Proc Royal Soc London B: Biol Sci* 266(1427):1403–1411.

25. Stavenga DG (2014) Thin film and multilayer optics cause structural colors of many insects and birds. *Materials Today: Proc* 1:109–121.

26. Trzeciak TM, Wilts BD, Stavenga DG, Vukusic P (2012) Variable multilayer reflection together with long-pass filtering pigment determines the wing coloration of papilionid butterflies of the nireus group. *Optics express* 20(8):8877–8890.

27. Ghiradella H (1991) Light and color on the wing: structural colors in butterflies and moths. *Applied optics* 30(24):3492.

28. Stavenga DG, et al. (2018) Classical lepidopteran wing scale colouration in the giant butterfly-moth Paysandisia archon. *PeerJ* 6:e4590.

29. Giraldo MA, Stavenga DG (2016) Brilliant iridescence of Morpho butterfly wing scales is due to both a thin film lower lamina and a multilayered upper lamina. *J Comp Phys A* 202(5):381–388.

30. Wahlberg N, et al. (2009) Nymphalid butterflies diversify following near demise at the Cretaceous/Tertiary boundary. *Proc Royal Soc B: Biol Sci* 276(1677):4295–4302.

31. Hafernik JE (1982) *Phenetics and Ecology of Hybridization in Buckeye Butterflies: Lepidoptera: Nymphalidae* (Univ of California Press, Berkeley).

32. Stoddard MC, Prum RO (2011) How colorful are birds? Evolution of the avian plumage color gamut. *Behav Ecol* 22(5):1042–1052.

33. Magkiriadou S, Park J-G, Kim Y-S, Manoharan VN (2014) Absence of red structural color in photonic glasses, bird feathers, and certain beetles. *Phys Rev E* 90(6):062302.

34. Nijhout HF (1991) *The development and evolution of butterfly wing patterns* (Smithsonian Institution Press, Washington).

35. Neild AF, D'Abrera B (2008) *The butterflies of Venezuela* (Meridian, London).

36. Pfeiler E, Johnson S, Markow TA (2012) DNA barcodes and insights into the relationships and systematics of buckeye butterflies (Nymphalidae: Nymphalinae: Junonia) from the Americas. *J Lep Soc* 66(4):185–198.

37. Gemmell AP, Borchers TE, Marcus JM (2014) Molecular population structure of Junonia butterflies from French Guiana, Guadeloupe, and Martinique. *Psyche: A Journal of Entomol* 2014:153-173.

38. Maia R, et al. (2013) pavo: an R package for the analysis, visualization and organization of spectral data. *Methods in Ecol & Evo* 4(10):906–913.

39. Joens MS, et al. (2013) Helium Ion Microscopy (HIM) for the imaging of biological samples at sub-nanometer resolution. *Scientific Reports* 3:3514.

40. Boden SA, Asadollahbaik A, Rutt HN, Bagnall DM (2012) Helium ion microscopy of Lepidoptera scales. *Scanning* 33:107-120.

41. Allen FI, et al. (2019) Gallium, neon and helium focused ion beam milling of thin films demonstrated for polymeric materials: study of implantation artifacts. *Nanoscale* 11:1403-1409.

Figure Legends

Figure 1: The lamina of a typical butterfly scale functions as a thin film reflector. *(A)* Colorized helium ion micrograph of a nymphaline scale, with a window milled using a gallium focused ion beam. Inset at higher magnification, with labels for general architectural components of a scale (R = ridges, r = cross-ribs, L = lower lamina). *(B)* Diagram of reflection and refraction in a chitin thin film. White light enters, reflections are produced at each surface of the film, and reflections of select wavelengths remain in phase as a function of film thickness (T). *(C)* Experimental disruptions of wing color are associated with altered lamina thickness. In *J. coenia,* artificial selection for blue color increased lamina thickness in both cover and ground scales. Some wing regions of *optix* mosaic knockout mutants have similar thickness increases. This trend recapitulates natural variation in *J. evarete*, where blue butterflies have thick laminae relative to brown individuals. (*** = $p < 1x10^{-7}$) Bars show mean thickness, with error bars of one standard deviation. *(D)* Wild-type *J. coenia. (E)* Blue artificially selected *J. coenia.* Image by Edith Smith. *(F) J. evarete.*

Figure 2: Structure and color of *Junonia* scales. *(A-D)* Artificially selected blue *J. coenia*. *(E-H)* Wild-type *J. coenia*. *(I-L) J. evarete*, blue male from Bolivia. *(M–P) J. evarete*, brown male from Jamaica. *(Q-T) optix* mosaic knockout mutant (mKO) in *J. coenia*. *(A,E,I,M,Q)* Dorsal hindwing, red arrowhead indicates the characterized scale's location. *(B,F,J,N,R)* Scale in the orientation it would occupy on the wing, showing the abwing surface of the cover scale. Black scale bars are 25 µm. *(B',F',J',N',R')* Adwing surface of cover scale, showing the underside of the lamina. *(B",F",J",N",R")* Dissected scale with arrow showing regions where all ridges and ribs are removed to expose the bare lamina. The lamina is sufficient to create iridescent blue and gold structural colors. *(B"',F"',J",N"',R"')* Scale immersed in fluid with a refractive index matched to chitin, thus eliminating refraction to show only pigmentary color. Blue and brown scales have comparable amounts of a brown pigment. *(C,G,K,O,S)* Helium ion micrograph of cross-sectioned scale. Each lamina is colorized, with approximate thickness indicated by an adjacent red bar (precise measurements were taken at sites chosen as in Methods). White scale bar is 500 nm and applies to all HIM images. *(D,H,L,P,T)* Reflection spectra for the adwing surface of disarticulated scales. Solid line is the mean spectrum, and blue envelope is one standard deviation; N=6 spectra per graph.

Figure 3: Absorbance spectra show the effect of artificial selection and *optix* knockout (mKO) on scale pigmentation. Pigment in cover scales is comparable across samples, indicating that pigment does not explain the color differences. *(A)* Absorbance measures in *J. coenia* wild-type (brown), artificially selected (blue), and *optix* mKO cover scales show that all have comparable pigmentation. Artificially selected scales have more variable absorbance, and both selected and

optix mKO cover scales have slightly higher mean absorbance than wild-type. *(B)* Absorbance of selected *J. coenia* ground scales is roughly doubled relative to brown wild-type scales. *optix* mKO ground scales also have increased pigmentation relative to wild-type. *(C)* Absorbance does not differ between blue and brown *J. evarete* cover scales, and is similar to pigmentation in *J. coenia* cover scales. Plots show mean spectra with envelope of one standard deviation, N=6 spectra per sample.

Figure 4: Lamina structural colors are an important component of overall wing color throughout *Junonia. (A)* Phylogeny of color variation in *Junonia* (based on [20]). Arrowheads indicate the color regions sampled for scale characterization. WT = wild-type. AS = artificial selection. mKO = *optix* mosaic knockout mutant. DS = winter/dry season form. WS = summer/wet season form. *J. evarete* variants are from different locations. Female *J. hierta* image is © Krushnamegh Kunte, NCBS. *(B,D,F,H,J,L)* Dorsal hindwing, arrow indicates the characterized scales' location. *(C,E,G,I,K,M)* Abwing surface of cover scale. *(C',E',G',I',K',M')* Adwing surface of cover scale, showing lamina color. *(C",E",G",I",K",M")* Scale immersed in fluid with refractive index matched to chitin, thus eliminating refraction and showing only pigmentary color. *(B-C") J. hierta* basal aura scales are unpigmented and appear blue due to lamina structural color. *(D-E") J. hierta* has coordinated yellow pigment with a structurally yellow lamina. *(F-G") J. atlites*. Despite being neutral light grey, color is exclusively structural, due to additive color mixing of the multicolored lamina. *(H-I")* Blue scales of dry season *P. octavia* are structurally colored since no pigment is present. *(J-K")* Wet season *P. octavia* has discordant red pigment and blue lamina colors. *(L-M")* The red band in dry season *P. octavia* is a more saturated red than in (H), due to the combination of both more red pigment and a structurally reddish lamina.

Figure 5: Lamina thickness predicts lamina color in wing regions across the *Junonia* phylogeny. *(A)* Thickness measures for the regions indicated in Fig. 4A show that thickness varies continuously over a 170 nm range (minimum N=3 scales and 12 measures per specimen). To visualize the relationship between thickness and color, we clustered similar specimens into five color groups described as gold, red, indigo, blue, and green. Thickness is significantly different between groups (ANOVA and Tukey's HSD, $p < 2x10^{-6}$). One sample with rainbow color gradients in each individual scale, *J. atlites*, has especially variable thickness, with measures overlapping the ranges of each color group. Boxplots show median and inner quartiles, whiskers extend to 1.5 times the interquartile range, outliers are shown as points, and notches show 95% confidence interval of the median. Violin plot shows that the overall distribution of lamina thickness for all samples is bimodal. *(B)* Color groups are also associated with different reflectance profiles. Lines are mean spectra; envelopes are one standard deviation. N=6 spectra per specimen from panel A; clusters follow panel A. *(C-F)* Adwing reflectance spectra for representative individual specimens with increasing lamina thicknesses. The color sequence follows Newton's series. Solid line is the mean spectrum and the envelope is one standard deviation; N=3 scales and 6 spectra per graph.

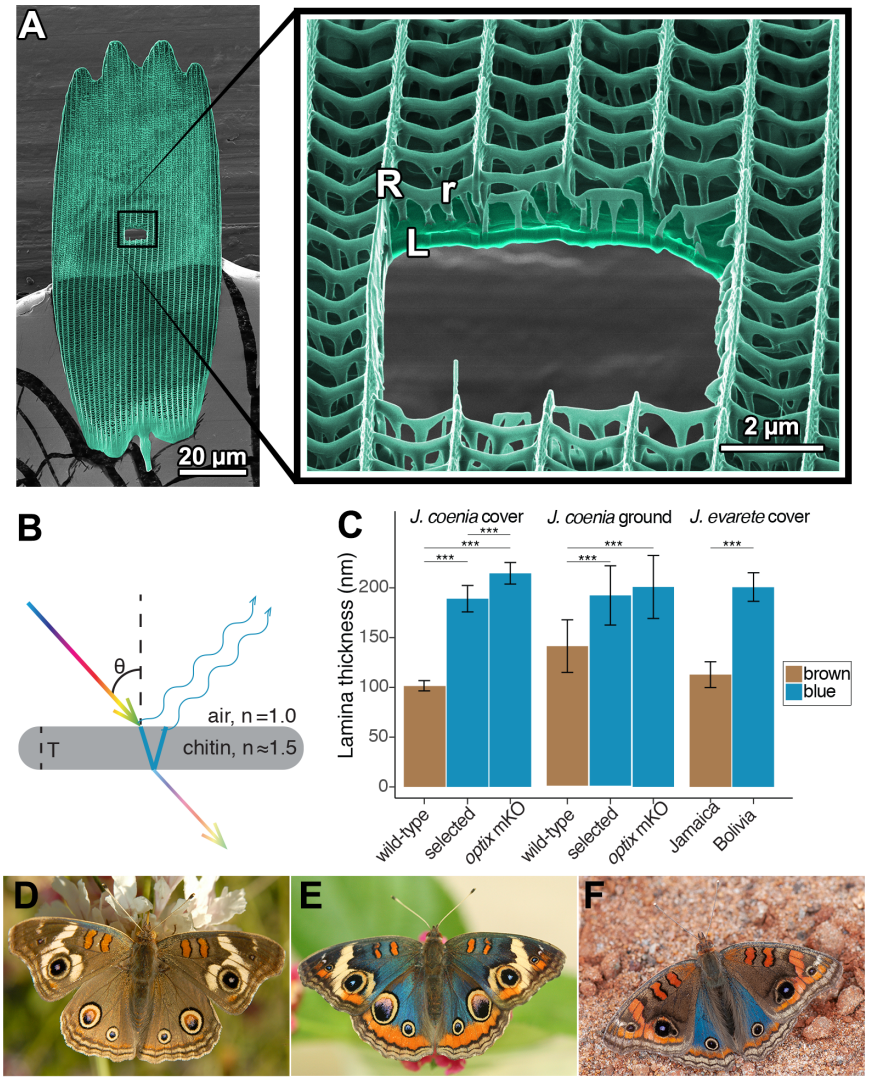
A
20 µm
R
r
L
2 µm
B
θ
air, n =1.0
T
chitin, n ≈1.5
C
J. coenia cover
J. coenia ground
J. evarete cover
Lamina thickness (nm)
0
50
100
150
200
***
brown
blue
wild-type
selected
optix mKO
wild-type
selected
optix mKO
Jamaica
Bolivia
D
E
F

Figure 1

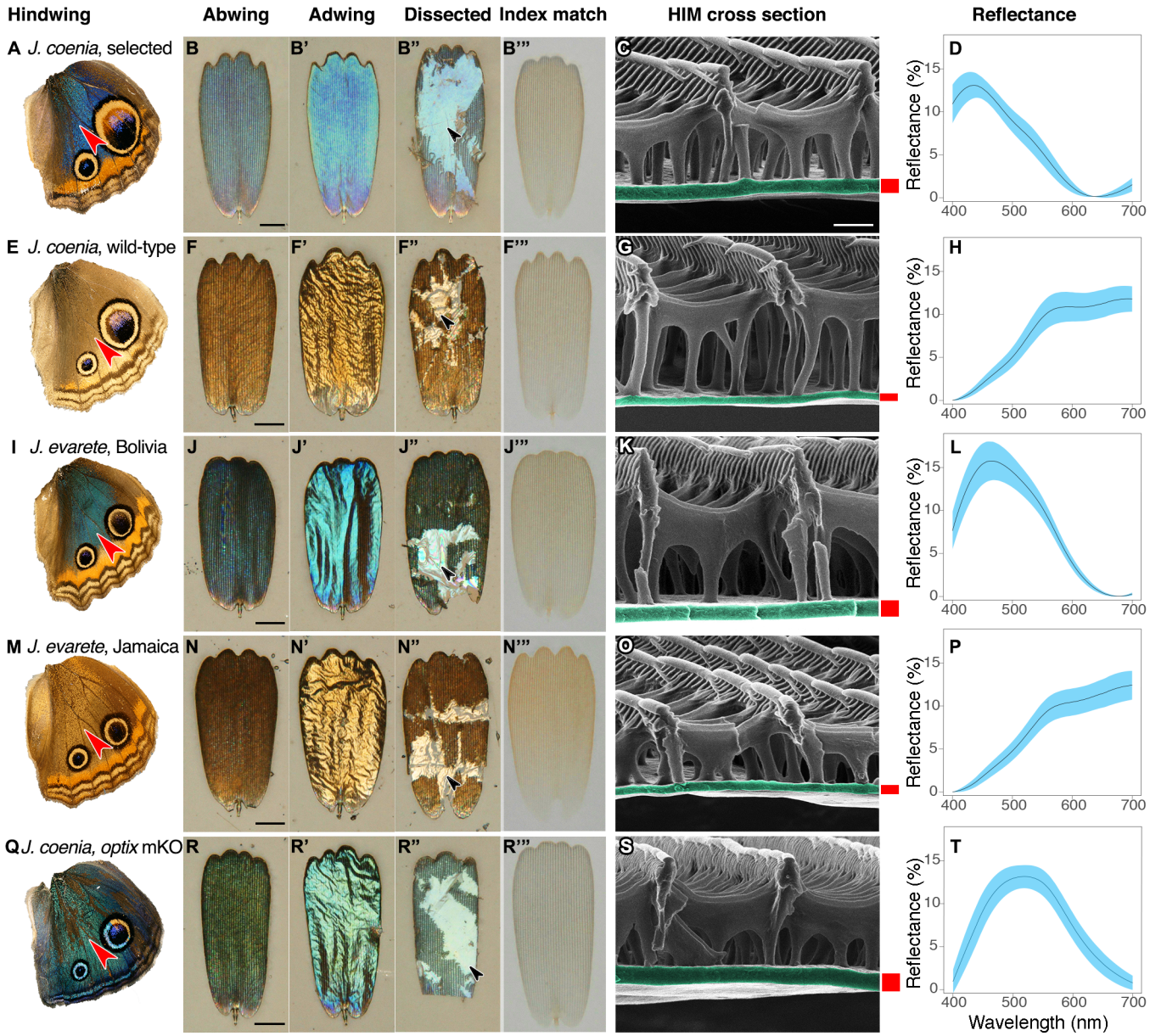
Hindwing
Abwing
Adwing
Dissected
Index match
HIM cross section
Reflectance
A J. coenia, selected
E J. coenia, wild-type
I J. evarete, Bolivia
M J. evarete, Jamaica
Q J. coenia, optix mKO
B
B'
B''
B'''
C
D
F
F'
F''
F'''
G
H
J
J'
J''
J'''
K
L
N
N'
N''
N'''
O
P
R
R'
R''
R'''
S
T
Reflectance (%)
0
5
10
15
400
500
600
700
Wavelength (nm)

Figure 2

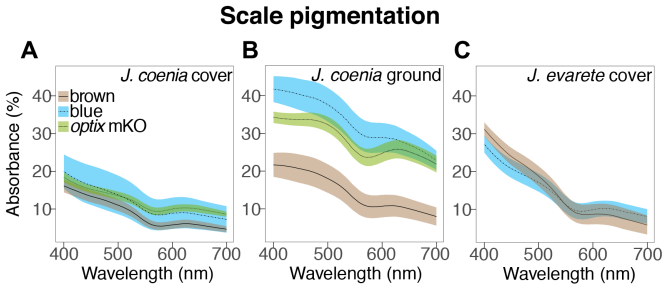
Scale pigmentation
A
B
C
J. coenia cover
J. coenia ground
J. evarete cover
brown
blue
optix mKO
Absorbance (%)
40
30
20
10
400
500
600
700
Wavelength (nm)

Figure 3

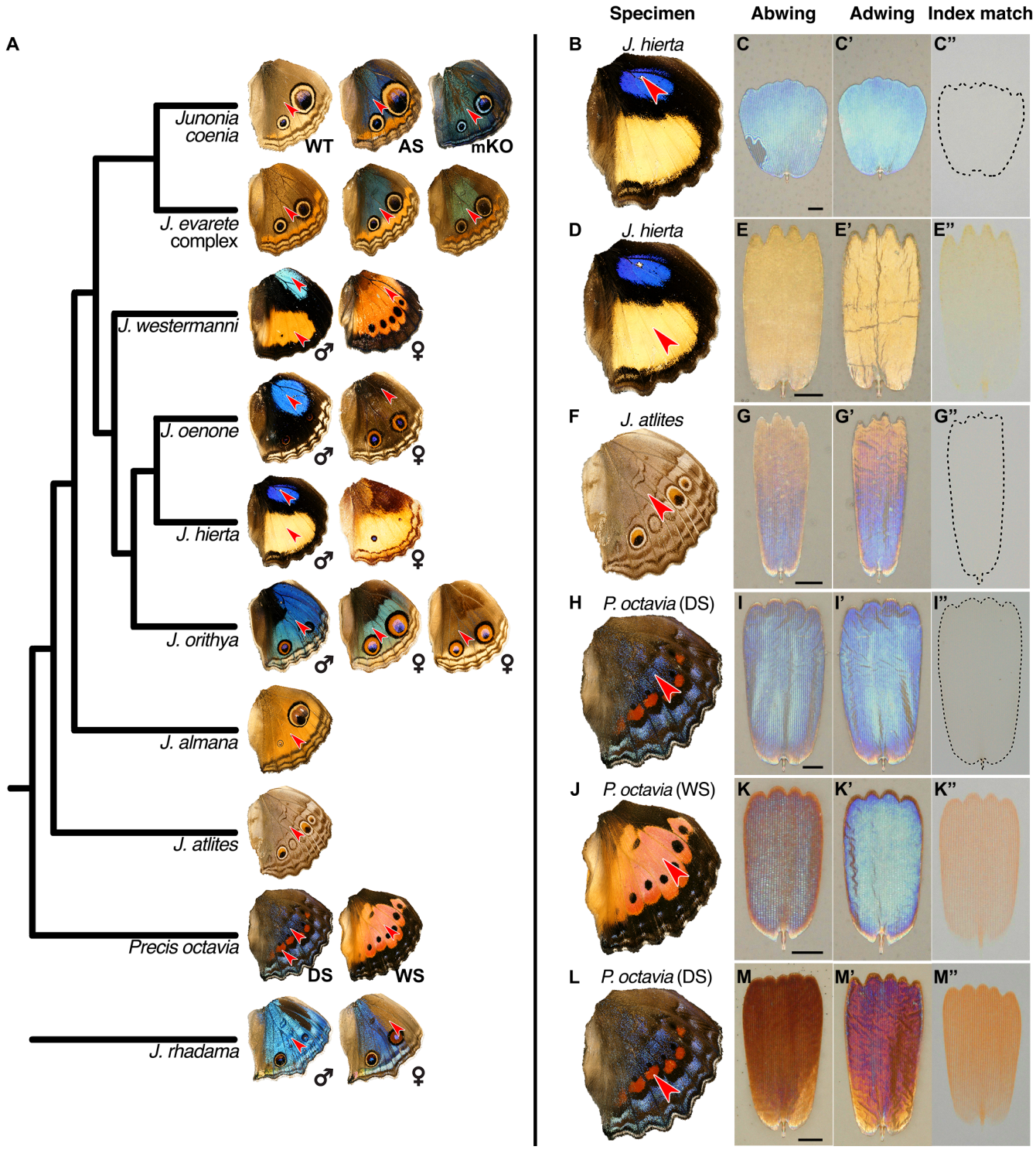
A
Junonia coenia
WT
AS
mKO
J. evarete complex
J. westermanni
J. oenone
J. hierta
J. orithya
J. almana
J. atlites
Precis octavia
DS
WS
J. rhadama
Specimen
Abwing
Adwing
Index match
B
J. hierta
C
C'
C''
D
J. hierta
E
E'
E''
F
J. atlites
G
G'
G''
H
P. octavia (DS)
I
I'
I''
J
P. octavia (WS)
K
K'
K''
L
P. octavia (DS)
M
M'
M''

Figure 4

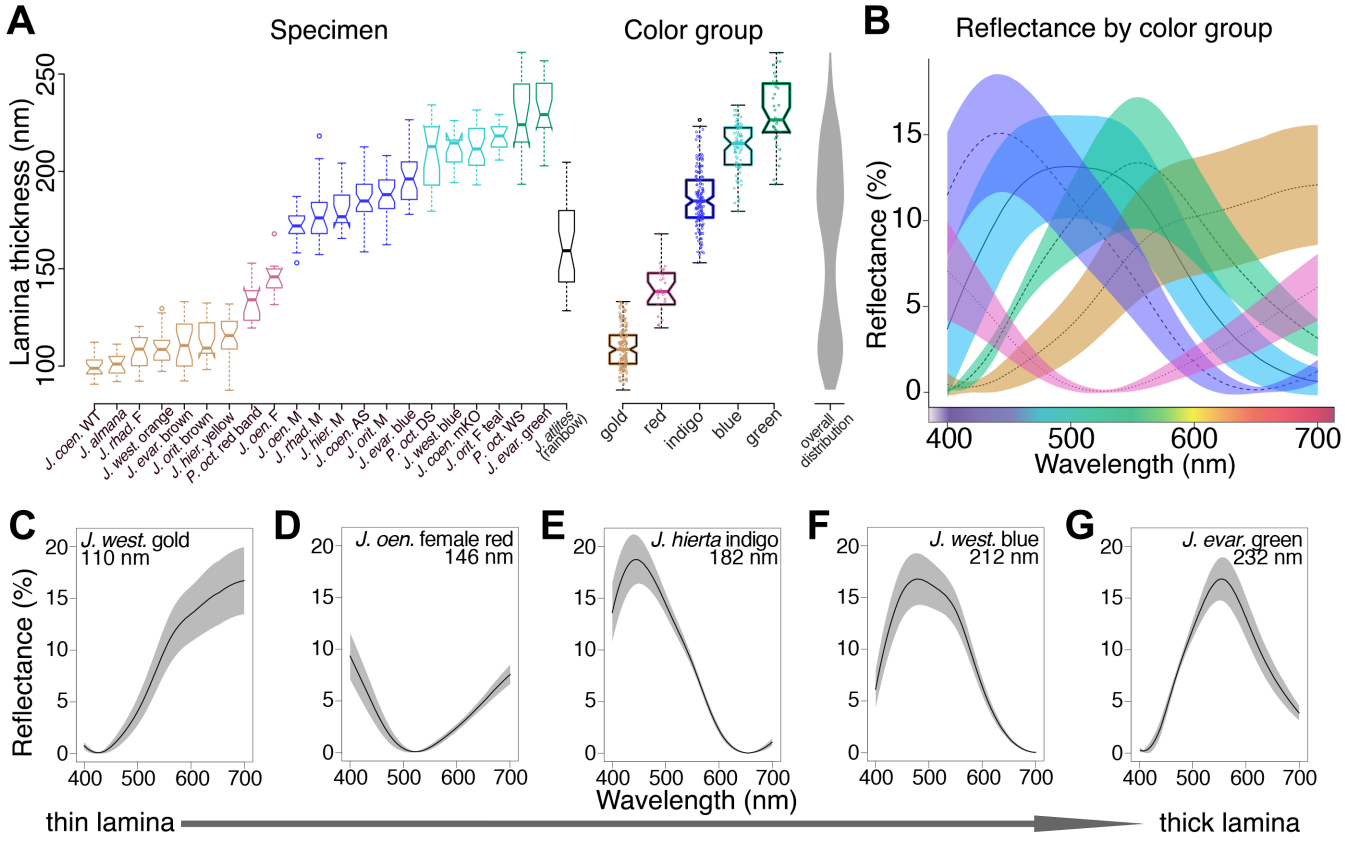
A
Specimen
Color group
Lamina thickness (nm)
100
150
200
250
J. coen. WT
J. almana
J. rhad. F
J. west. orange
J. evar. brown
J. orit. brown
J. hier. yellow
P. oct. red band
J. oen. F
J. oen. M
J. rhad. M
J. hier. M
J. coen. AS
J. orit. M
J. evar. blue
P. oct. DS
J. west. blue
J. coen. mKO
J. orit. F teal
P. oct. WS
J. evar. green
J. atlites (rainbow)
gold
red
indigo
blue
green
overall distribution
B
Reflectance by color group
Reflectance (%)
0
5
10
15
400
500
600
700
Wavelength (nm)
C
J. west. gold
110 nm
D
J. oen. female red
146 nm
E
J. hierta indigo
182 nm
F
J. west. blue
212 nm
G
J. evar. green
232 nm
Reflectance (%)
Wavelength (nm)
thin lamina
thick lamina

Figure 5